The Use of Ground-Penetrating Radar To Map the Buried Structures and Landscape of the Ceren Site, El Salvador

Lawrence B. Conyers

Department of Anthropology, University of Colorado, Campus Box 233, Boulder, Colorado, 80309-0233

More than 7800 m of digital ground-penetrating radar data were acquired at the buried 6th century archaeological site of Ceren in El Salvador. The data were used to explore for buried structures and map the paleotopography through more than 5 m of volcanic overburden. The archaeological site consists of an agricultural village that was rapidly buried by pyroclastic debris erupted from a nearby volcano, preserving structures, plants, agricultural fields, and much of the surrounding landscape. Ground-penetrating radar profiles were computer-processed to remove system and background noise and time-depth corrected to identify the reflection which represents the ancient ground surface. This buried surface, and the structures built on it, were computer-modeled in two dimensions to aid in anomaly identification and interpretation. Twenty-six buried structures were identified on GPR profiles and an accurate representation of the landscape and environment, as it existed just prior to the eruption, was reconstructed. Ground-penetrating radar is an excellent geophysical tool with which to reconstruct buried landscapes and map cultural features due to its ability to accurately resolve underground features in three dimensions.

INTRODUCTION

Ground-penetrating radar (GPR) has been employed with increasing success during the last two decades to explore for and map buried archaeological sites. One of the benefits of the method is that raw reflection data can be viewed in the field and anomalies, which may represent buried archaeological features, can be identified. In this fashion ground-penetrating radar has primarily been used by archaeologists to identify and prioritize areas for future archaeological excavation or conservation.

With the advent of digital GPR, and the application of velocity analysis to these data, radar reflection data can now be computer-processed and radar wave travel times converted to depth. Anomalies cannot only be identified as to their nature, but the depth and orientation of important cultural features can be mapped. Digital data can also be readily computer processed to enhance and filter the reflected signal, allowing greater definition and clarity of subsurface reflections. In this study more than 7800 m of digital GPR data, acquired

over the buried 6th century agricultural village of Ceren in El Salvador (Figure 1), have been analyzed. Structures buried by as much as 6 m of pyroclastic debris have been located, the topography of the ancient living surface has been mapped, and prehistoric land uses have been identified. A three-dimensional picture of the landscape which surrounds the houses, and the delineation of the extent of the village, have been studied noninvasively.

THE CEREN SITE

The Ceren site consists of a prehistoric agriculturally oriented village of more than 30 buildings which was buried by pyroclastic debris about 1400 years ago (Sheets, 1992). It is located approximately 25 kilometers northwest of the capital city of San Salvador in the Zapotitan Valley (Figure 1). The volcanic eruptions that buried the site led to unusually good preservation of almost all cultural materials, including buildings and their contents, as well as plants which grew in surrounding agricultural fields and orchards. Four areal excavations have been conducted to date which have totally or partially uncovered 16 structures and agricultural fields and gardens. Each of the excavations reveal, through small "windows" excavated into the pyroclastic overburden, an almost complete array of artifacts and ecofacts, which tell a great deal about small portions of the 6th century world of El Salvador.

All excavated buildings were constructed of adobe with thatch roofs (Kievit, 1994). Households consisted of multiple structures of various uses, clustered together into units where families or extended families lived. Each household cluster was separated from the others by gardens and agricultural fields, and connected by footpaths. Most prehistoric structures at Ceren are located on natural topographic rises which were raised further on a foundation of baked clay (Kievit, 1994). Domicile buildings and storage houses (bodegas) have puddled-earthen columns on all four corners with wattle-and-daub "bajareque" walls between columns. Other civic or communal buildings are more substantial with thick earthen walls and interior platforms and benches.

Agricultural fields, orchards, and household gardens have been encountered in many excavations. Maize, numerous trees, and other plants were encountered as hollow cavities, which are preserved as casts when the cavities are filled with dental plaster during excavation.

The richness of the archaeological data from the excavations stand in stark contrast to the lack of knowledge about the regional environment and landscape of the area prior to the eruption. Detailed mapping of the landscape and cultural features using ground-penetrating radar indicates that at least 22 previously unknown structures are present in the area that has not yet been excavated. The surrounding unexposed portion of the archaeological site, which has not yet been explored geophysically, likely covers many tens of hectares.

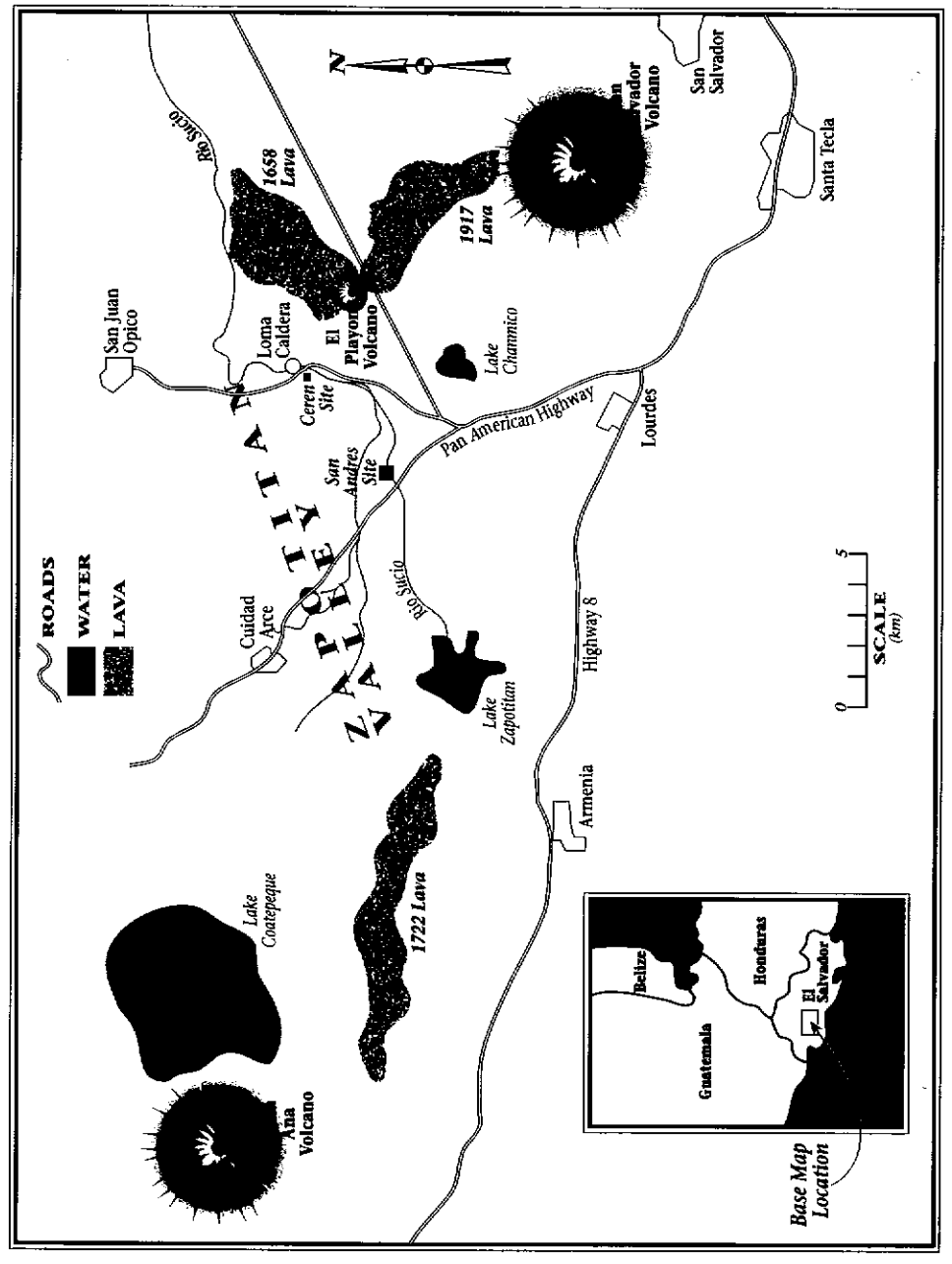

Figure 1. Location of the Ceren Site, El Salvador.

GPR METHOD AND THEORY

The GPR method involves the transmission of high-frequency electromagnetic radio pulses into the earth and measures the time elapsed between transmission, reflection off a subsurface discontinuity, and reception back to the surface radar antenna. As the antennae are moved along the ground surface, a continuous profile of subsurface reflections is constructed. The propagation velocity of the electromagnetic waves through the earth depends on a number of factors, the most important ones being the electrical properties of the material through which they pass (Olhoeft, 1981). When the velocity of the waves through the material is known, the travel time of radar pulses can be converted to depth.

Ground-penetrating radar waves radiate electromagnetic energy into the ground in a conical shape with the apex of the cone at the center of the transmitting antenna. Radiation fore and aft from the antenna is usually greater than to the sides, making the illumination pattern on a subsurface plane elliptical in shape, with the long axis of the ellipse parallel to the direction of antenna travel (Annan and Cosway, 1992). The subsurface radiation pattern is therefore always "looking" not only directly below the antenna but also in front, behind, and to the sides.

When the velocity of electromagnetic pulses traveling in the ground changes, usually at a subsurface interface, a portion of the radar energy is reflected back to the surface and recorded at the receiving antenna. The amplitude of the reflected waves is approximately proportional to the magnitude of the velocity change at the interface. Received signals are then amplified, demodulated, and recorded either on paper by a graphic recorder, on magnetic tape in the audio frequency range, or digitally on a computer hard-disk drive or tape.

The maximum effective depth of radar wave penetration is a function of the frequency of the radar waves and the physical characteristics of the material through which they are traveling. Higher frequency radar waves (300–2000 MHz) have very good subsurface reflection resolution, but do not penetrate deeply. The maximum depth of penetration for a 500-MHz radar wave is only about 3 m under optimum conditions. Lower frequency GPR antennae (40–300 MHz) can produce radar energy with a depth penetration approaching 20 m, but resolution of buried features is sacrificed.

Ground-penetrating radar signal attenuation occurs as waves pass through the earth. Attenuation is influenced primarily by the electrical conductivity of the material through which the radar energy passes. Materials such as dry sand or porous volcanic tephra, which have a low electrical conductivity, allow greater electromagnetic energy propagation. In highly conductive materials such as moist clays, electromagnetic waves are dispersed and the signal is attenuated.

The presence of a water-saturated medium also has an effect on radar signal attenuation. Water molecules are bipolar and will rotate and become aligned with an electromagnetic field. Molecular rotation causes the radar energy to be converted to mechanical energy which is then dissipated as heat (Olhoeft, 1994). This loss of energy, which is frequency-dependent, is referred to as dielectric relaxation.

Relative dielectric permittivity (RDP) is a measure of the ability of a material within an electric field to become polarized and therefore respond to propagated electromagnetic waves (Olhoeft, 1981). The RDP of a material is defined as the dimensionless ratio of its electrical permittivity to the permittivity of a vacuum (which is 1). Dielectric permittivities of materials vary with composition, moisture content, bulk density, porosity, physical structure, and temperature. The RDP of dry sand is approximately 5, water-saturated sand has an RDP between 20 and 30, and the RDP of clay can approach 40 (Davis and Annan, 1989).

The primary goal of many archaeological GPR investigations is to differentiate subsurface interfaces. All sedimentary layers and buried archaeological features have particular electrical properties that affect the velocity of electromagnetic signal propagation, as measured by RDP. The reflectivity of radar energy at an interface is primarily a function of the magnitude of the difference in RDP between the two materials on either side of the interface. The greater the contrast in electrical properties, the greater the velocity change, and the stronger the reflected signal (Sellmann et al., 1983). Electrical property changes are caused primarily by changes in water content, which create the boundaries that reflect radar energy (Olhoeft, 1984). In settings above the ground water table, moisture content changes are usually coincident with bed or feature boundaries. Subsurface reflections visible on GPR profiles are therefore directly controlled by changes in radar wave velocity, which are primarily caused by changes in water content.

THE EVOLUTION OF GROUND-PENETRATING RADAR IN ARCHAEOLOGICAL MAPPING

One of the first applications of GPR to archaeological exploration was conducted at Chaco Canyon, New Mexico (Vickers and Dolphin, 1975). These surveys were successful in discovering the location of buried walls under dry sandy soils at depths ranging from 1 to 2 ft. Other early GPR successes included the discovery of buried barn walls and storage cellars in Pennsylvania (Bevan and Kenyon, 1975; Kenyon, 1977) and collapsed and standing walls in Cyprus (Fischer et al., 1980).

During 1982 and 1983 GPR surveys were carried out at the Red Bay, Labrador archaeological site in Canada in an attempt to locate graves, buried artifacts, and house walls associated with a 16th century Basque whaling village (Vaughan, 1986). Discovered GPR anomalies were later excavated and found to represent disturbed soil around graves and structure walls made of beach cobbles.

A comprehensive series of GPR surveys were conducted in Japan in the mid-1980s to locate buried 6th century A.D. houses, burial mounds, and cultural layers (Imai et al., 1987). In these studies GPR surveys proved capable of resolving the sunken floors of ancient dwellings which were buried, in some cases, by 2 m of pumice and loamy soil. Velocity analyses were performed which allowed two-way travel time to be converted to depth. After the GPR investigations were complete, approximately 12,000 sq m of one site were excavated. The locations of radar anomalies were then compared to the locations of houses, burial mounds, and associated trenches, with excellent correlation. Three cultural layers, which were defined by burial soil horizons and dated by associated stone artifacts, were delineated on some GPR profiles as distinct reflections.

Success in time-depth conversions of GPR profiles made velocity analyses more common in the late 1980s and early 1990s, which allowed the depth to archaeologically significant features to be quantitatively mapped. In most cases, however, "anomaly hunting" or projection of known features into the subsurface was still the primary goal of most archaeologists (Bailey, 1987; De Vore, 1990; Stove and Addyman, 1989; Roosevelt, 1991).

Early GPR successes in Japan were followed by additional archaeological surveys which discovered and mapped buried kilns, burial mounds surrounded by moats, and individual stone-lined burials (Goodman and Nishimura, 1993; Goodman et al., 1994; Goodman, 1994). These studies pioneered the use of many novel GPR techniques including time and depth slice maps (Goodman, 1994), computer simulated two-dimensional models, and three-dimensional reconstructions of buried features (Goodman and Nishimura, 1993).

The use of GPR in archaeological exploration has advanced dramatically over the last 20 years. The ability to convert reflections, measured in time, to approximate depth using calibrations derived from velocity analyses was a major advancement (Vaughan, 1986; Imai et al., 1987). The definition of reflections which correspond to horizons of archaeological interest was also important in the reconstruction of buried topography (Imai et al., 1987).

INITIAL GROUND-PENETRATING RADAR SURVEYS AT CEREN

The use of GPR at the Ceren site in 1979 (Loker, 1983; Sheets et al., 1985) was one of the first archaeological applications of this method. A subsurface interface radar system (SIR-7) with a single 80 MHz antenna, mounted about 10 cm above the ground, was attached to the rear of a cart pulled by two oxen. The survey was conducted in early June, after almost 7 months with little or no rain, so that the ground was extremely dry. A total of 40 traverses were made, spaced every 5 m, to create a grid of just a little less than 1 ha of ground surface. Radar reflection data were printed out on paper with a graphic recorder and recorded on FM magnetic tape (Loker, 1983). One anomaly was discovered on paper copies of raw reflection data, which at the time appeared to represent

an arching of tephra, perhaps over a buried structure. The anomaly was later tested by drilling and found to be a buried structure (Loker, 1983).

In 1992 additional GPR data were acquired at the site (Doolittle and Miller, 1992). Due to high ground moisture when the survey was made (August, which is midrainy season), radar energy was attenuated between 2 and 3 m, and no anomalies of significance were identified.

SITE STRATIGRAPHY

The oldest stratigraphic unit exposed at Ceren is a dark reddish-brown clay (Figure 2). This clay unit is the weathered upper portion of a regional volcanic ash unit erupted from the Coatepeque Caldera about 30 km southwest of Ceren between 10,000 and 40,000 years ago (Sheets, 1983). Directly overlying this basal clay is a white fine-grained volcanic ash layer (Figure 2), which has been given the informal name "Tierra Blanca Joven" (young white earth) or TBJ for short (Hart and Steen-McIntyre, 1983). The TBJ ash was erupted from the Ilopango Volcano, east of the city of San Salvador, about A.D. 260 ± 114. Its thickness varies between 30 and 40 cm at the Ceren site. The slightly weathered TBJ was the living surface upon which the ancient village of Ceren was constructed. There is abundant evidence of cultivation in the form of ridges and furrows within preserved agricultural fields in the upper portion of the ash. The underlying clay was used as construction material for the building of structures and surfacing of plazas and patios in the ancient village (Kievit, 1994) and was mixed with the TBJ in some agricultural fields (Zier, 1983).

The eruption which buried the ancient village of Ceren occurred about A.D. 590 ± 90 (Sheets, 1983), encasing the village with a thickness of as much as 6 m of tephra (Miller, 1989, 1990, 1992, 1993). A series of pyroclastic units from this eruption, termed the Ceren Sequence (Figure 2), lies directly on the TBJ surface, or the underlying clay where the TBJ was removed or eroded. In general, the Ceren Sequence consists of an alternating succession of pyroclastic-surge units and airfall block and lapilli deposits (Miller, 1989). The source for these units has been located about 600 m north of the site at what is now a highly eroded tuff-ring called Loma Caldera (Miller, 1992).

RECENT GROUND-PENETRATING RADAR ACQUISITION, PROCESSING AND INTERPRETATION

Acquisition and Processing

Approximately 4000 m of raw GPR reflection data, recorded in 1979 and saved on magnetic tape, were digitized as part of this study. In addition, approximately 3800 m of digital GPR data was acquired in 1994 using both 300 and 500 MHz dual antennae and a SIR-10 radar instrument. The total GPR data base at the site consists of more than 7800 m of GPR data in five grids, covering approximately 2 ha of surface area.

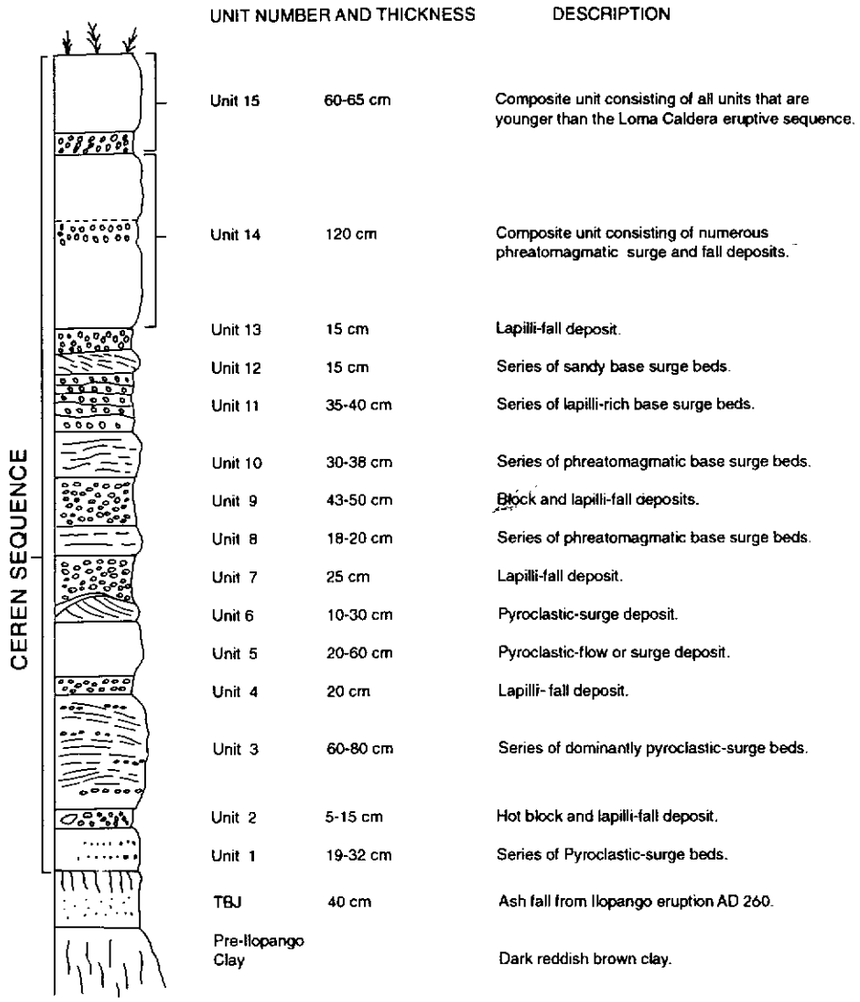

Figure 2. Stratigraphic section at the Ceren Site. (Modified from Miller, 1989)

The 1979 GPR data, which cover approximately 1 ha, were acquired before the majority of the archaeological excavations. The buried living surface has now been exposed in approximately 4% of the GPR grid area, allowing many features visible on GPR profiles to be directly compared to known archaeological and topographic features.

The 80-MHz data digitization process converted the analog reflection data, recorded as varying voltage changes on magnetic tape, to numerical values.

These data were then computer processed to filter out background noise, and the signal was enhanced to create profiles for all lines in the initial survey.

During data acquisition in 1994 all reflection data were recorded digitally on computer tape. Computer stacking of traces was done during acquisition. Depending on the speed with which the antennae were transported across the ground, either eight or sixteen successive traces were arithmetically stacked into each recorded trace. The degree of subsurface reflector definition is proportional to both the number of sequential traces stacked and the speed at which the radar antenna sled is dragged across the ground. When the antennae are moved slowly, more data can be acquired every second and a higher stack can be applied. When moving at a faster rate, lower stacks are necessary to ensure good subsurface coverage along each GPR traverse. Stacking of successive traces is also necessary to decrease random and incoherent noise, which can obscure important reflective events. It also reduces recorded signals that may have been caused by anomalous surface or subsurface irregularities.

Gain control and band-pass filters were employed during the 1994 data acquisition. Gain control is a method of amplifying reflections that are received from subsurface interfaces. This amplification procedure compensates for the radar energy lost by attenuation as it travels through the ground. Band-pass filters were used so that only those data frequencies between approximately 75 and 500 MHz were recorded. Frequencies higher than 500 MHz, which can be caused by FM radio transmission or electrical currents nearby, were filtered out. Low frequencies, which may represent system noise inherent to the radar instruments, were also filtered out during this procedure.

The 80 MHz grid, acquired in 1979, was not surveyed, and therefore no topographic corrections were possible due to ground surface modification during the last 10 years. A review of topographic maps produced for the site just after the 1979 GPR survey showed that maximum topographic variation across the 1-ha grid was a little less than 1 m. For this reason topographic corrections for the 80-MHz GPR grid were not attempted. All GPR grids acquired in 1994 were surveyed and corrections were made for surface topography.

Time-Depth Analysis

A number of methods were employed to convert two-way GPR travel time to depth. In the most accurate and straightforward method, radar data were acquired over known objects at known depths, which allowed for direct depth conversion of two-way travel time.

The first direct field test performed at the site involved the detection of a 2.5 cm diameter iron bar. The bar was pounded into the side of a pit exactly 1.1 m below the ground surface. The 500 MHz antennae were placed at the ground surface and slowly pulled over the metal bar while radar waves were projected into the subsurface. A hyperbola created by subsurface reflections off the metal bar was recorded, with the apex of the hyperbola, representing the iron bar, located at 13 ns (two-way time).

Another time-depth test was performed in a test pit where the corner of a buried structure had been partially excavated. A 2 m long portion of the structure's wall was 2.51 m below the ground surface. The 300 MHz profile, which perpendicularly crossed the wall, recorded a distinct reflection at the top of the wall at 38 ns (two-way time).

Using the equation relating time to depth for radar wave propagation (Davis and Annan, 1989), radar travel times can be converted to depth and velocities and relative dielectric permittivity of the overburden can be estimated:

$$K^{1/2} = \frac{C \times T/2}{D}$$

D = vertical depth or distance in meters
C = speed of light (0.2998 m/ns)
T = travel time of each radar pulse (from the antenna to the reflector and back to the antenna) (ns)
K = relative dielectric permittivity (RDP) of the material through which the radar pulse passes

The velocities and relative dielectric permittivities obtained from these tests are shown in Table I. These analyses indicate that radar wave velocity decreases slightly with depth. The decrease is probably caused by increasing residual moisture, which can increase radar travel times. Overall, the estimated velocities through the Ceren Sequence tephra are quite high, comparable to that of dry sand, which has a measured velocity of about 15 cm/ns (Davis and Annan, 1989).

Correlation of GPR Reflections to Stratigraphy

To correlate radar reflections visible in GPR profiles to known stratigraphy, two GPR profiles were acquired that abutted test pits at each end (Figure 3). Between the two test pits the 300 MHz antennae were used to acquired GPR data to a depth of approximately 5 m. Data collected with the 500 MHz antennae resolved bedding features from the surface to about 3 m.

The highest amplitude and most continuous reflector on this profile is visible at 62 ns (two-way time) on the western edge of the line (Figure 3). An estimated depth for the discontinuity which likely created the reflection, using the average velocity of 13.2 cm/ns obtained from the test on the wall, is 409 cm. The only significant lithologic discontinuity visible in the test pit at this depth was the contact between the TBJ ash and the overlying Ceren Sequence tephra, located at 420 cm. In nearby test pits and excavations the TBJ–tephra interface is the location of small moisture seeps, especially during the rainy season. The upper portion of the TBJ ash is compact and retains moisture while the overlying tephra is more porous and permeable and relatively dry. The high amplitude radar reflection was therefore likely generated by a lithologic and moisture change at this interface, located within 11 cm of the depth estimated using a velocity of 13.2 cm/ns. Interpretation of more than 7800 m of GPR data within all the Ceren GPR grids has demonstrated that the elevation of this high amplitude reflection accurately represents all known topographic features on the TBJ surface. This is also the most archaeologically important reflector because it represents the ancient living surface prior to its burial by pyroclastic debris about A.D. 590.

Other reflections, visible in both the 300 and 500 MHz data, can also be correlated to specific tephra units measured in both test pits (Figure 3). Unit 8 is the most indurated tephra unit in the Ceren Sequence, which also retains the most moisture. It can be correlated between pits (Figure 3), confirming the stratigraphic correlations and velocity measurements.

Using velocities derived from correlating the TBJ reflection to the known stratigraphy in both test pits allows a calculation of a relative dielectric permittivity of 4.9 for the Ceren Sequence as a whole. This is very similar to that which was calculated in the test on the buried wall (Table I). This RDP was used during all time-depth conversions.

Table I. Velocity analysis results from the bar and wall tests.

Depth (meters)	Total Distance (cm.)	Ceren Seq. Unit No.	Two-Way Time (ns)	RDP	Velocity (cm/ns)
0–1.1 (bar)	220	13–8	13	3.14	16.92
0–2.51 (wall)	502	13–3	38	5.15	13.21

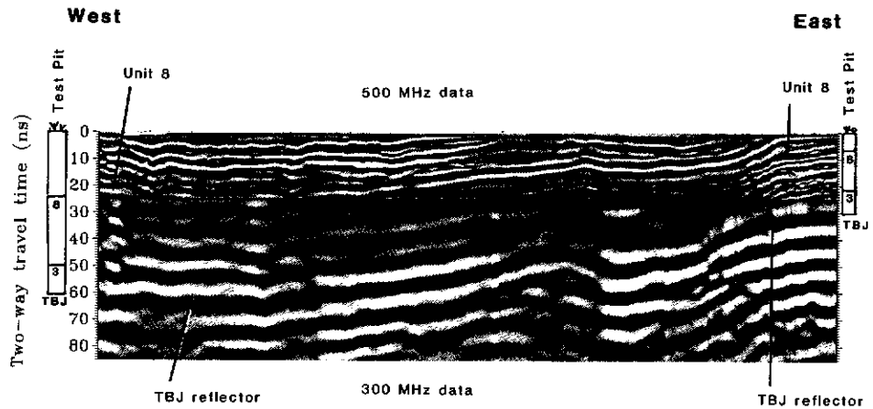

Figure 3. 500- and 300-MHz GPR profiles which tie test pits on either end. Tops of stratigraphic layers which were measured in test pits are shown on either end of the profiles. (The profile is 12.5N in Grid 3, just east of Operation 2).

It is probable that the imposition of only one relative dielectric permittivity, derived from only one area of the site, to all Ceren GPR data may have yielded spurious depth calculations in areas where subsurface conditions may differ from the test areas. For instance, greater depths to the TBJ in some areas would theoretically allow for a greater amount of moist tephra overburden, lowering the average velocity of waves traveling to and from the surface. The TBJ would then appear in GPR profiles to be too shallow because a higher average velocity was assumed during data processing. Conversely areas where the TBJ is located in a higher than average paleotopographic position would have less tephra overburden and a correspondingly lower overall moisture. This condition would increase the average velocity of radar waves through the tephra, but because a RDP of 4.9 was imposed upon the section (derived from an area with lower average velocities), the TBJ would actually be closer to the surface than indicated on GPR profiles. A more geographically dispersed velocity calibration set would allow for more accurate time–depth conversions throughout the area, but the errors introduced by these variations are probably not great.

Interpretation of the GPR Data

GPR profiles are two-dimensional displays of all reflection traces plotted along an acquisition line. When two-way travel time is converted to depth, the profiles can be considered an approximate representation of a shallow slice through the earth along each transect. The profiles of each GPR line appear to be an accurate cross-section of the earth. Actually each cross-section is a "distorted pseudo-section" (Olhoeft, 1994), with the most distinct portion of each reflection probably representing radar energy reflected from directly below. The cone-shaped radar beam which is radiated from the surface antenna also allows for transmission to, and reflection from, subsurface discontinuities outside of the vertical plane that passes through the receiving and sending antennae. As a result, data recorded at any one location on the surface may include radar energy that was reflected from in front and in back, as well as to the sides of the line being surveyed.

The time it takes a radar pulse to travel to and from a subsurface discontinuity which is not directly below the GPR unit is usually greater than the time it takes a radar wave to travel directly down and then back up. When time is converted to depth, reflections which were not derived from directly below the antenna appear to be at a greater depth than they actually are. As a result, when reflection data from all traces in a line are plotted in two dimensions, the reflection record of any subsurface discontinuity becomes "smeared." This smearing occurs as reflections are received at the antenna from multiple points on the same horizon within the radius of the transmission cone. Reflection events are therefore not as distinct as one would like, and subsurface resolution decreases. This can be partially overcome by employing a higher frequency antenna with a narrower cone of transmission (Annan and Cosway, 1992), but depth penetration is sacrificed.

When anomalous objects or "point sources" such as buried structures or other features are encountered, disruption of the usual radar reflections occurs. Some waves, which have been radiated as much as 45° in front and behind the transmitting antenna, will strike the buried object along a slanted ray path, returning to the receiving antenna along the same path. This is especially true with 80 MHz data, which has a wider cone of radiation than that produced by the 300 or 500 MHz antennae. The receiving antenna records these reflections as if they were being received from directly below. The distance that the nonvertical reflected waves travel, and therefore their measured times, are longer than waves which traveled directly down and back. As the radar antenna moves over the ground surface and the buried object becomes closer, the apparent depth, as measured by the time of the nonvertically traveling waves, becomes less and less. When the GPR unit is directly over the object, radar reflection time is at a minimum. As the antennae moves past the buried object the process reverses itself and the object appears at greater apparent depths. When the series of all these traces received from the buried structure are printed in a two-dimensional profile, the resulting reflection forms a hyperbola.

In this study these hyperbolic reflections, indicating the presence of a significant buried feature, are referred to as "point source reflections." Because the radar beam is conical, point source reflections are received from not only in front and behind the antenna, but also from discontinuities located to the side. Many buried cultural features therefore can be distinguished by point source reflections generated in any direction from the antenna, and their appearance on a number of GPR profiles is usually necessary for accurate mapping.

Synthetic GPR Models

Synthetic radargram modeling was developed in an attempt to model, within a two-dimensional plane, buried objects and reflection surfaces. This modeling can show what real-world GPR data should look like under ideal circumstances (Goodman and Nishimura, 1993; Goodman, 1994; Cai and McMechan, 1994). Computer-simulated models trace the paths of rays during transmission and reflection through various media with specific relative dielectric permittivities. The models take into account reflectivity coefficients encountered at various interfaces, signal attenuation, and relative dielectric permittivities of units (Goodman, 1994).

Ray-path models are based on a complex series of calculations using conductive–dissipative electromagnetic propagation theory (Jackson, 1977). The reflected amplitude responses are then predicted, and two-dimensional GPR reflection simulations are created. These simulations can be made for a number of frequency antennas and relative dielectric permittivities to approximate the real-world case being modeled. The resulting models can then be compared with actual field data to provide support for interpretation.

Two synthetic radargrams were created to model an area around one representative structure at the Ceren site (Figure 4). In all models relative dielectric

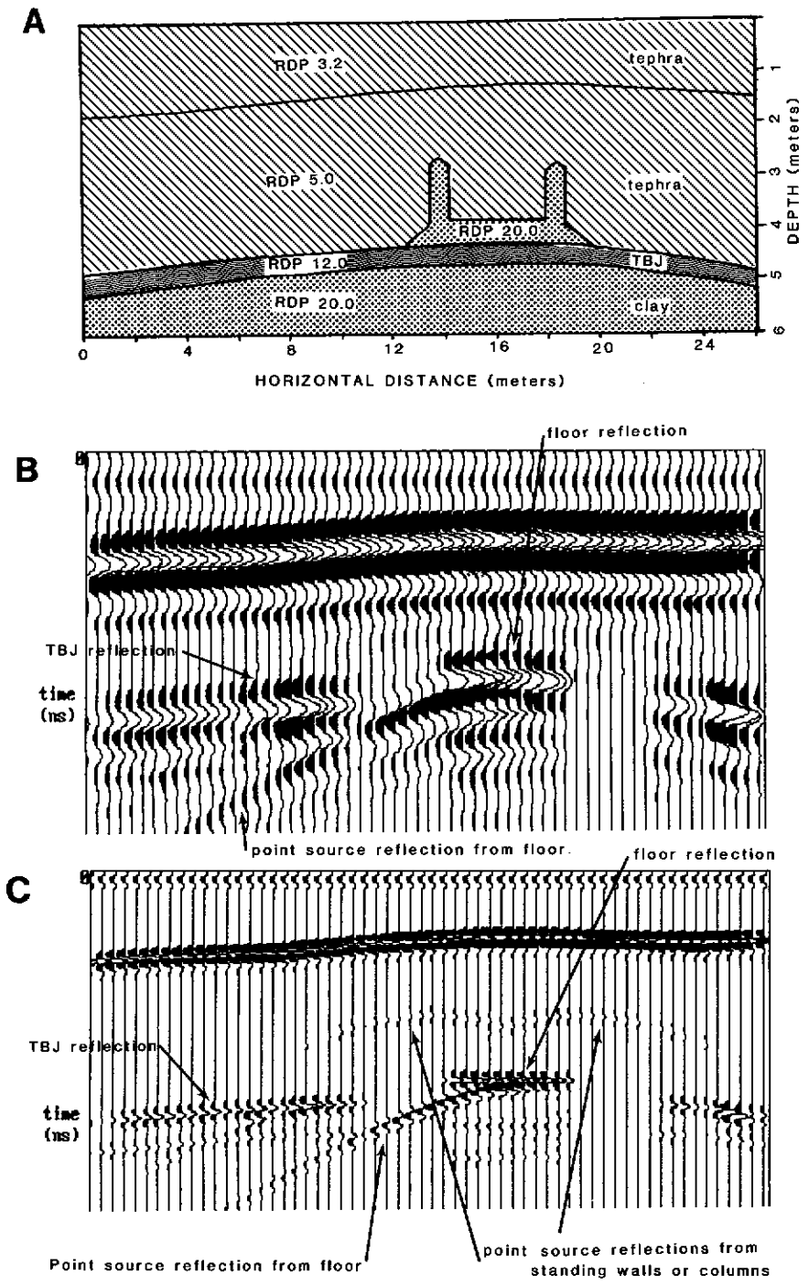

Figure 4. Two-dimensional synthetic radar models: (A) modeled structure built on the TBJ surface with estimated RDP for archaeological features and stratigraphic layers; (B) 80-MHz model show-

permittivities, as obtained from field tests were employed. A RDP of 3.2 (similar to the RDP obtained in the bar test) was used for Ceren Sequence tephra layers from the surface to a depth of 2 m. This represents Ceren Sequence Units 15 to about the top of Unit 9. The RDP between 2 and 5 m depth was increased from 3.2 to 5.0 (similar to the RDP obtained in the wall test). The RDP differences which likely exist between specific tephra units and a gradual increase in RDP with depth were not simulated.

The computer modeled a significant change in RDP at the Ceren Sequence-TBJ contact from 5 to 12 due to increasing water saturation, compaction, and clay content. The TBJ thickness was modeled at 40 cm, with no lateral dimension changes.

A structure with two standing columns and walls was simulated on a topographic rise, covered by about 3 m of tephra (Figure 4). The structure was modeled after Structure 2, now excavated (Kievit, 1994), which is visible on three of the 80 MHz GPR profiles. The structural platform, walls, and columns were assumed to have the same RDP as the clay unit underlying the TBJ (RDP = 20), based on the knowledge that structures were constructed of clay mined primarily from that unit (Kievit, 1994). A moderate amount of tephra bowing was assumed over the buried structure, as observed during its excavation (McKee, 1989).

Computer computations used to construct the models begin by simulating the directions radar waves would have taken within a two-dimensional grid. Beginning amplitudes and directions are specified by the program (Goodman, 1994). The model predicts the degree of transmission and reflection within the media and the relative amplitudes of reflected waves generated at bed boundaries from the RDP data input. When computer-simulated rays are reflected back to the surface, their locations and amplitudes are recorded.

Both the 80 and 300 MHz models indicate that a high amplitude reflection will occur at the tephra–TBJ interface, replicating what is seen in GPR sections at the site (Figure 4). The models also indicate that a strong point-source reflection would be created from the floor of the structure. The simulations illustrate how the reflections from the floors of buried structures will obscure the underlying TBJ reflection. This phenomenon is visible on many GPR lines which cross structures (Figure 5).

Computer-generated models were used as a basis for interpreting the radar profiles from all GPR grids. A remarkable similarity exists between what the models predict and what was visible in many GPR sections, adding a large degree of confidence to many of the interpretations discussed below.

MAPPING OF BURIED TOPOGRAPHY AND IDENTIFICATION OF BURIED STRUCTURES

During radar profile interpretation, the TBJ reflector, first identified along the test line (Figure 3), was identified on each profile and "tied" at each line intersection to assure consistency. Subsurface elevations of the TBJ were then

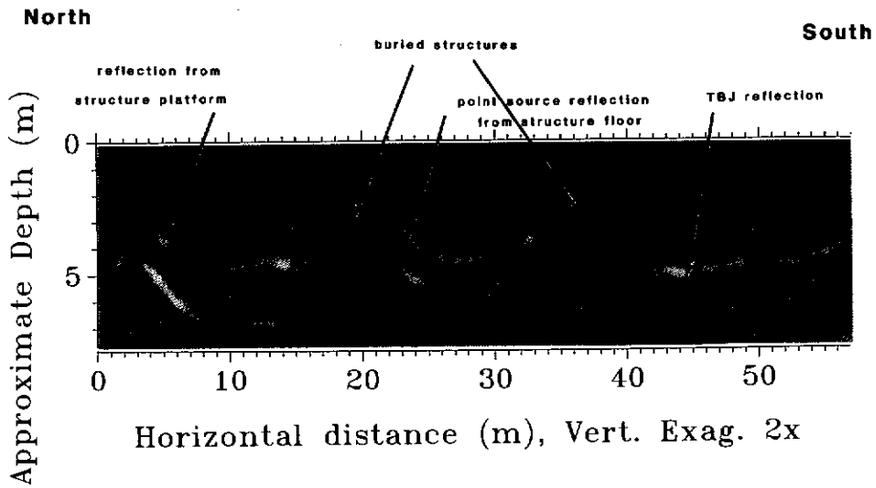

Figure 5. 80-MHz frequency GPR profile across three buried structures. (The profile is 75E in Grid 1.)

contoured to reveal the topography of the buried living surface just prior to the eruption (Figure 6).

Archaeological investigations have shown that the ancient living surface prior to the Loma Caldera eruption was not always the top of the TBJ ash. In some excavations the TBJ was found to have been paved with a layer of clay in plaza and patio areas (Gerstle, 1992). In others it had been totally removed, either by erosion or human action. Many times the TBJ ash was found to have been mixed with clay, especially in areas which were heavily cultivated (Zier, 1983) or in the vicinity of structures where clay was used in construction (Kievit, 1994). For these reasons what was mapped as the TBJ reflection may in some locations be the top of the underlying clay or the top of a unit of mixed TBJ ash and clay. The lack of resolution which could distinguish these kind of lithologic differences, all of which occur within a 40–50 cm layer, precludes further differentiation. Therefore, when discussing the "TBJ reflector," a lithologic unit, in the geologic sense, is not implied. The horizon mapped as TBJ, however, in all cases was the living, working, farming, and construction surface, just prior to the Loma Caldera eruption, irrespective of local variations in lithology.

All point-source reflectors visible in GPR profiles, which may denote buried structures or other subsurface anomalies, were recorded during profile interpretation (Figure 6). As demonstrated in the synthetic models, point source reflections are derived from the tops or sides of structural platforms and from the tops of walls or columns. Reflections generated from house platforms are very

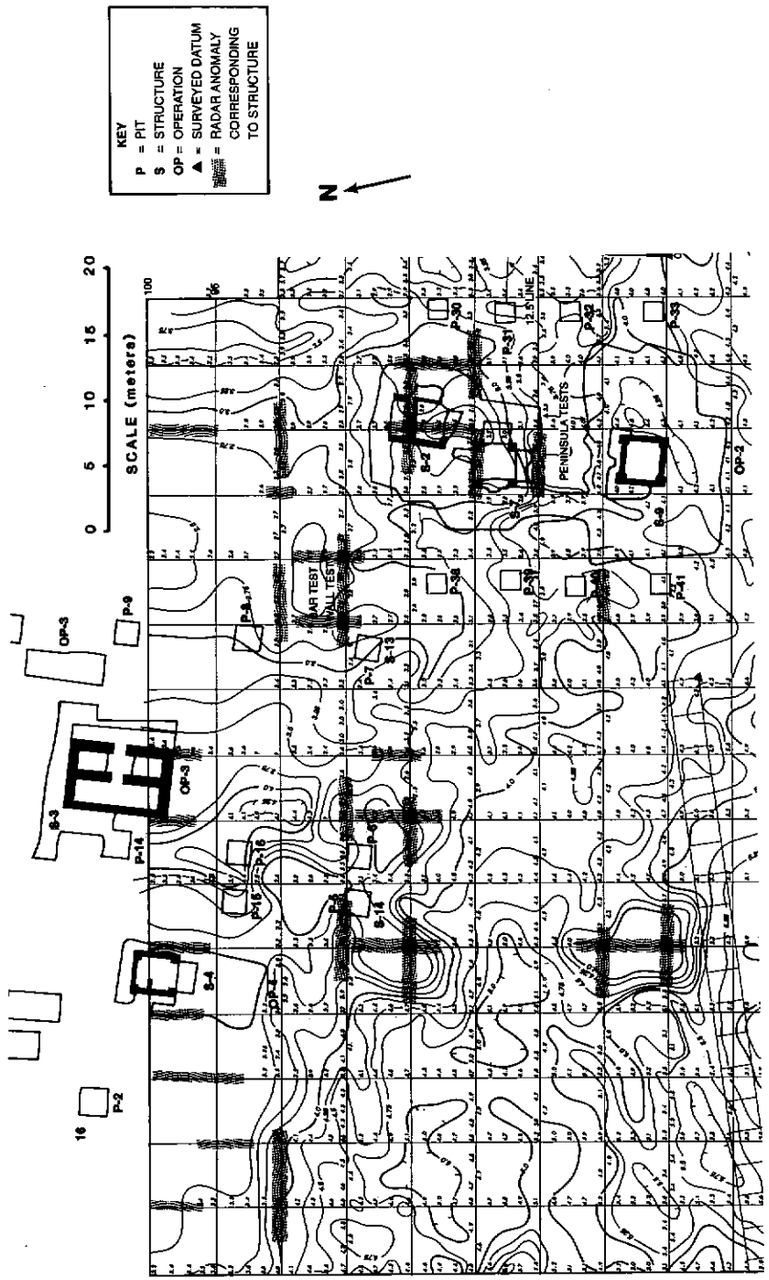

distinct on 80 MHz profiles while those from the top of standing walls or columns are so subtle that they are almost invisible.

Distinctive point source reflections with apexes above the clay floors of structures are, in contrast, readily visible on the 300 MHz data (Figure 7). The apexes of these reflections are a little more than 1 m above the clay floor surface, similar to the height of many standing columns in some excavated structures (Kievit, 1994). It is probable that they were generated from the tops or sides of standing columns or walls, as predicted in the two-dimensional synthetic models (Figure 4). Point source reflections from clay floors also occur in 300 MHz data, but are less common than in 80 MHz data. They were not recorded farther than about 1 m away from the clay foundation reflection surfaces, probably because the radar beam of the 300 MHz antenna is more narrow (Annan and Cosway, 1992) and is thus not capable of "seeing" the anomaly as far in advance or behind the unit. The correlation between point-source reflections and the location of structure platforms known from excavation is excellent. Of the nine excavated or partially excavated structures located within the GPR grids, eight can be readily identified by point source reflections and mappable rises in the local topography. Eighteen additional structures are identifiable in GPR profiles that have yet to be confirmed by drilling or excavation.

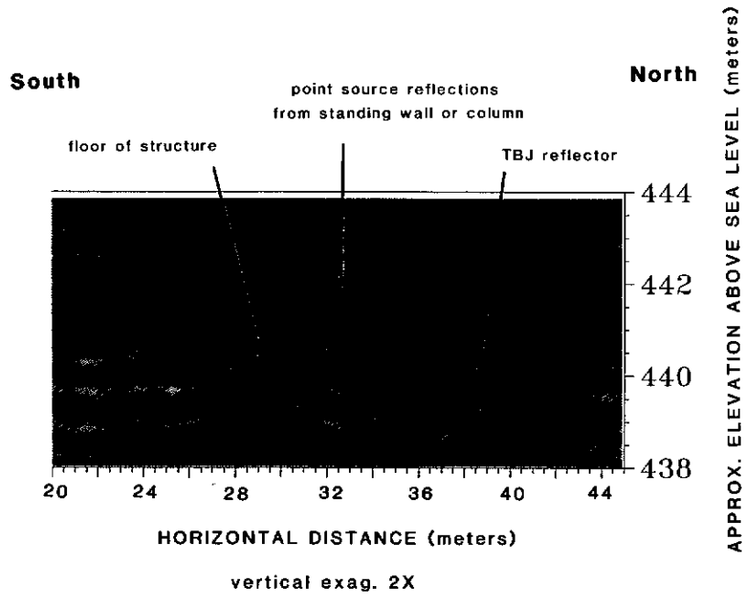

Figure 7. 300-MHz frequency GPR profile across a buried structure with possible standing walls or columns. (The profile is 10.0E in Grid 4.)

The 300 MHz data are capable of resolving subtle changes in topography at the TBJ horizon associated with the construction of foundations (Figure 7). The total foundation height of some buried structure platforms, which is at most about 20 cm, cannot be discerned in the 80 MHz data but is readily visible on 300 MHz profiles.

THE VILLAGE AND LANDSCAPE OF CEREN

Mapping of the TBJ living surface, and locating structures built upon it, were accomplished by constructing paleotopographic contour maps of the buried landscape and identifying reflection anomalies generated from buried structures (Figure 6). All structure locations, as defined during archaeological excavations or as mapped by GPR, are identified. The most striking feature of the buried TBJ surface is the variation in topography across the site and the intricacy of the buried drainage pattern.

To produce a visual image of the ancient landscape, a computer-generated three-dimensional picture of the TBJ surface was constructed (Figure 8). A data base of 3130 TBJ elevations, each measured in meters above sea level every 1.25 m along each line within the GPR grids, was used. The imaging program that created this image applied a "minimum curvature" arithmetic algorithm that created a "best-fit" surface to the subsurface data points. The image does not include the buried structures built on this topographic surface.

In general, the landscape, just prior to the Loma Caldera eruption, consisted of a small elongated valley, located in the west-central portion of the GPR grids, surrounded by low bluffs to the north and east. A gradual southern slope rose out of the valley to the southeast, ultimately forming a large hill to the south. Buried structures are located primarily on the northern and southern flanks of the central valley. Within the central valley were located a complex series of drainage channels, geographically restricted topographic rises and small closed depressions. Drainage channels within the valley had a maximum depth of about 1.5 m. Their banks were gently sloping with no discernable cutbanks. The numerous small closed depressions and mounds within channels in the central valley were probably created by clay quarrying operations.

Archaeological observations from excavations and pits along the northern portion of the GPR grids allows for the categorization of space usage and landscape patterns at the site. Some of these patterns can be projected into the subsurface with the aid of GPR-produced topographic maps of the buried living surface, yielding a map of the cultural landscape. Figure 9 includes both features that are known from the excavations and those that have been projected into the subsurface with the aid of GPR data. The map illustrates the preference of the inhabitants for building structures on the north flank of the valley. This area was also the location of numerous other use areas including "in-field" gardens (Killion, 1992), orchards, and small maize fields that have been excavated (Sheets, 1992).

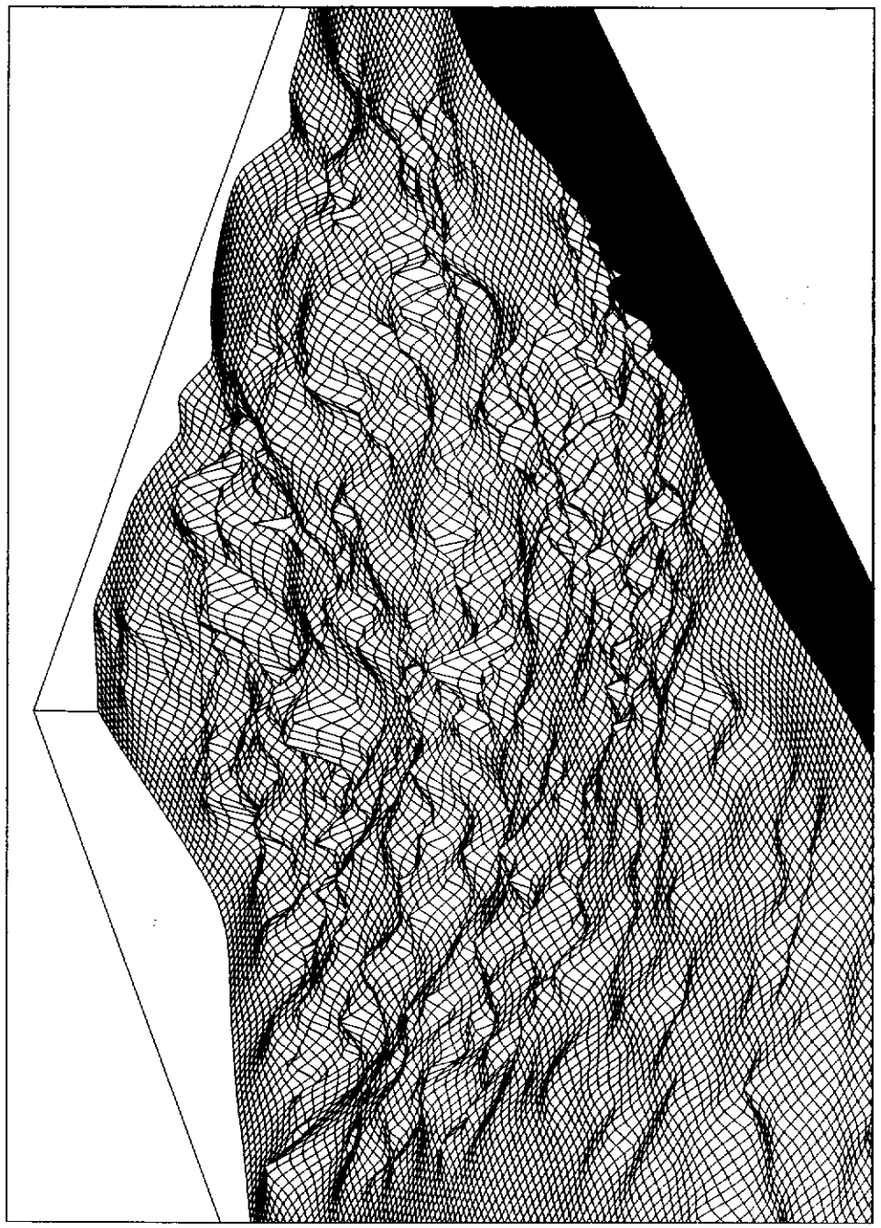

Figure 8. Three-dimensional image of the buried TBJ living surface. The image is viewed from the southeast at an angle of 20° from the horizontal. All topographic features are exaggerated five times.

The plaza, located on the crest of the bluff on the north edge of the valley (Figure 9), was surrounded on the east, south, and west by structures which probably had a civic function (Sheets, 1992). The plaza can be identified on many GPR profiles as a high-amplitude flat reflective surface. The northern edge of the plaza was destroyed during the 1976 bulldozing operations, and its northern boundary is not known.

Three household clusters and numerous scattered houses are visible on GPR profiles within the northern portion of the radar grids. Their abundance in a relatively small area indicates that the population density at Ceren was quite high at the time of the eruption (Figure 9). The presence of the plaza and its associated communal buildings, as well as the religious structures just to the east of the GPR grids (Sheets, 1992), is evidence for the presence of many more people than conceivably could have lived in the households so far identified in excavations and the GPR surveys.

Ceren was likely a small village consisting of at least 40–50 families. The village was agriculturally oriented as shown by the nearby fields, the agricultural tools stored in structures, and the bodegas for food storage (Sheets, 1992). The plaza and other civic and religious buildings indicate that the north part of the village was probably the focal point of the community. Other buildings that were likely part of the village, but have yet to be discovered, are probably located to the northwest and west of the known extent of the site.

CONCLUSION

The accurate identification and mapping of the topography of the buried living surface at Ceren was achieved only after time–depth conversions were performed. This allowed the ancient living surface reflector to be identified and its subsurface elevation to be measured. The paleotopographic maps produced from these elevations illustrate the complex nature of the buried living surface. The abundance of channels and ridges between household clusters was startling to many of us who had preconceived ideas of a relatively unvarying paleotopography. Only after GPR mapping of the site could the archaeological richness derived from excavations be integrated into its ancient landscape.

This study demonstrates that the ancient village of Ceren was constructed around a small valley, located between bluffs. Houses were constructed on the highest topographic areas, and the valley bottom was likely the location of agricultural activitiy and clay quarrying. No excavations have been conducted in the valley, and to the south, and therefore specific activities that might have been conducted there must remain speculative.

The southern boundary of the village was discovered near the southern edge of radar Grid 1. Land devoted to agriculture was likely located south of this area, although this has not yet been confirmed by excavation. The presence of a large plaza and surrounding civic buildings to the north of the central valley, which are visible on GPR profiles, indicates that the ancient community of Ceren was probably the focus of activity for a large number of people who lived

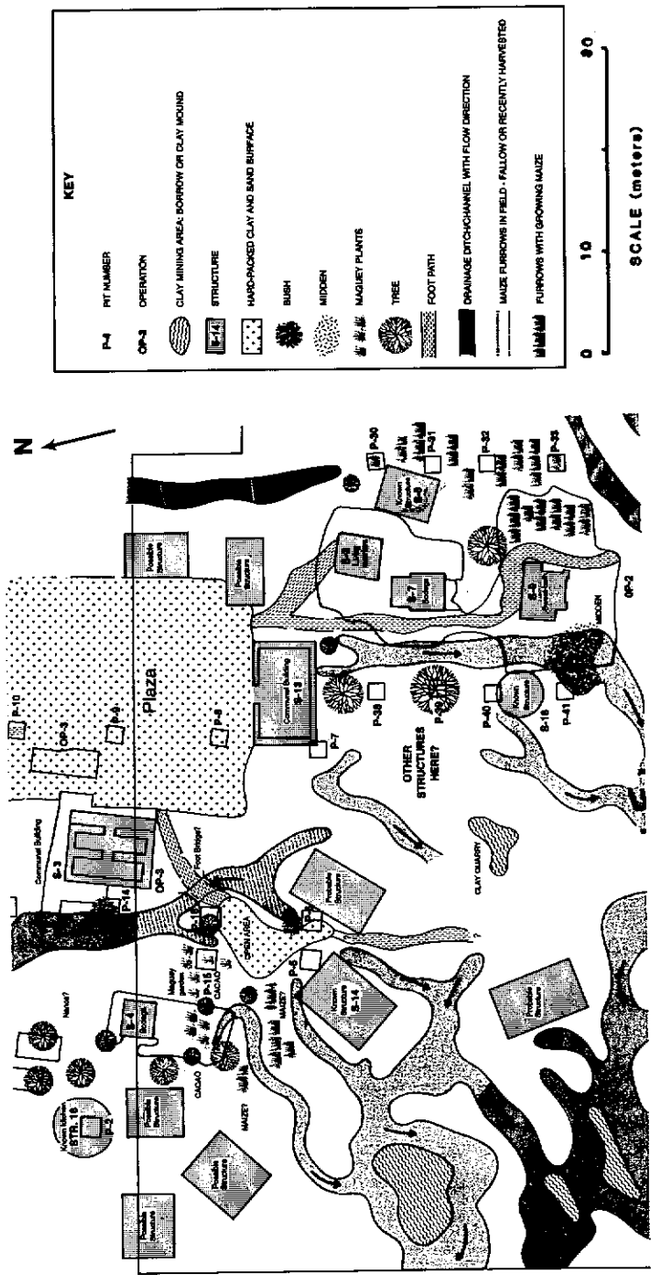

Figure 9. Cultural features visible on GPR profiles and projections of features from excavated areas.

nearby. The radar mapping shows that the density of structures within the village was very high. At least 36 structures are known from excavations or have been mapped geophysically within an area of a little less than 1 ha. The buildings located by archaeological excavation and GPR are probably only a small percentage of the total that still remain undetected to the northwest and west of the present site. Only future GPR work accompanied by archaeological excavation will be able to confirm its extent in those directions.

Many archaeologists who use GPR are primarily concerned only with identifying buried anomalies that represent features of interest. This study shows how ground-penetrating radar gives archaeologists the ability to noninvasively map not only buried structures and other cultural features, but also the ancient landscape of a site.

Many thanks go to Jeff Lucius at the U.S. Geological Survey in Golden, Colorado, and Gary Olhoeft at the Colorado School of Mines for their assistance in data gathering and processing. Some of the GPR equipment used in the field was loaned by Geophysical Survey Systems, Inc. of North Salem, New Hampshire and the U.S. Geological Survey. The two-dimensional synthetic models were constructed by Dean Goodman. Many thanks for help during data acquisition and interpretation go to Payson Sheets. David Tucker aided in field acquisition and surveying. Bill Miller constructed the three-dimensional visual image of the buried living surface. Payson Sheets, Mike Powers, and three anonymous reviewers commented on earlier drafts of this article.

REFERENCES

Annan, A.P., and Cosway, W.W. (1992). Simplified GPR Beam Model for Survey Design. Extended Abstract of 62nd Annual International Meeting of the Society of Exploration Geophysicists, New Orleans, October 25–29.

Bailey, R.A. (1987). Subsurface Interface Radar at Sepphoris, Israel, 1985. *Journal of Field Archaeology* **14**(1), 1–8.

Bevan, B., and Kenyon, J. (1975). Ground-Penetrating Radar for Historical Archaeology. *MASCA Newsletter* **11**(2), 2–7.

Cai, J. and McMechan, G.A. (1994). Ray-Based Synthesis of Bistatic Ground Penetrating Radar Profiles. *In Proceedings of the Fifth International Conference on Ground Penetrating Radar*, pp. 19–29. Waterloo, Canada: Waterloo Centre for Groundwater Research.

Davis, J.L., and Annan, A.P. (1989). Ground-Penetrating Radar for High-Resolution Mapping of Soil and Rock Stratigraphy. *Geophysics* **37**, 531–551.

De Vore, S.L. (1990). Ground-Penetrating Radar as a Survey Tool in Archaeological Investigations: An Example from Fort Laramie National Historic Site. *The Wyoming Archaeologist* **33**(1–2), 23–38.

Doolittle, J.A., and Miller, F. (1992). Geophysical Investigations at the Ceren Site, El Salvador. *In* P.D. Sheets and K.A. Kievit, Eds., *1992 Investigations at the Ceren Site, El Salvador: A Preliminary Report*, pp. 10–19. Boulder: Department of Anthropology, University of Colorado.

Fischer, P.M., Follin, Sven G.W., and Ulriksen, P. (1980). Subsurface interface radar survey at Hala Sultan Tekke, Cyprus. *In* Peter M. Fischer, Ed., *Applications of Technical Devices in Archaeology*, pp. 48–51. *Studies in Mediterranean Archaeology* 63. P. Astrom: Goteborg, Sweden.

Gerstle, A. (1992). Test Excavations in Joya de Ceren, 1990–1992: Operations 3, 4, 6 and 7. Unpublished manuscript on file. Boulder: Department of Anthropology, University of Colorado.

Goodman, D. and Nishimura, Y. (1993). A Ground-Radar View of Japanese Burial Mounds. *Antiquity* **67**, 349–354.

Goodman, D., Nishimura, Y., Uno, R., and Yamamoto, T. (1994). A Ground Radar Survey of Medieval Kiln Sites in Suzu City, Western Japan. *Archaeometry* **36**(2), 317–326.
Goodman, D. (1994). Ground-Penetrating Radar Simulation in Engineering and Archaeology. *Geophysics* **59,** 224–232.
Hart, W.J.E., and Steen-McIntyre, V. (1983). Tierra Blanca Joven Tephra from the AD 260 Eruption of Ilopango Caldera. *In* P.D. Sheets, Ed., *Archaeology and Volcanism in Central America,* pp. 35–43. Austin: University of Texas Press.
Imai, T. Sakayama, T. and Kanemori, T. (1987). Use of Ground-Probing Radar and Resistivity Surveys for Archaeological Investigations. *Geophysics* **52,** 137–150.
Jackson, J.D. (1977). *Classical Electrodynamics.* New York: John Wiley.
Kenyon, J.L. (1977). Ground-Penetrating Radar and Its Application to a Historical Archaeological Site. *Historical Archaeology* **11,** 48–55.
Kievit, K.A. (1994). Jewel of Ceren: Form and Function Comparisons for the Earthen Structures of Joya de Ceren, El Salvador. *Ancient Mesoamerica* **5**(2), 193–208.
Killion, T.W. (1992). Residential Ethnoarchaeology and Ancient Site Structure: Contemporary Farming and Prehistoric Settlement Agriculture at Matacapan, Veracruz, Mexico. *In* T.K. Killion, Ed., *Gardens of Prehistory: The Settlement Agriculture in Greater Mesoamerica,* pp. 119–149. Tuscaloosa: University of Alabama Press.
Loker, W.A. (1983). Recent Geophysical Explorations at Ceren. *In* P.D. Sheets, Ed., *Archaeology and Volcanism in Central America,* pp. 254–274. Austin: University of Texas Press.
McKee, B. (1989). Excavations at Structure Complex 2. *In* P.D. Sheets and B.R. McKee, Eds., *1989 Archaeological Investigations at the Ceren Site, El Salvador: A Preliminary Report,* pp. 41–58. Boulder: Department of Anthropology, University of Colorado.
Miller, C.D. (1989). Stratigraphy of Volcanic Deposits at El Ceren. *In* P.D. Sheets and B.R. McKee, Eds., *1989 Archaeological Investigations at the Ceren Site, El Salvador: A Preliminary Report,* pp. 8–19. Boulder: Department of Anthropology, University of Colorado.
Miller, C.D. (1990). Stratigraphy of Volcanic Deposits at Ceren: 1990. *In* P.D. Sheets and B.R. McKee, Eds., *1990 Archaeological Investigations at the Ceren Site, El Salvador: A Preliminary Report,* pp. 18–26. Boulder: Department of Anthropology, University of Colorado.
Miller, C.D. (1992). Summary of 1992 Geological Investigations at Joya de Ceren. *In* P.D. Sheets and K.A. Kievit, Eds., *1992 Archaeological Investigations at the Ceren Site, El Salvador: A Preliminary Report,* pp. 55–60. Boulder: Department of Anthropology, University of Colorado.
Miller, C.D. (1993). Summary of 1993 Geological Investigations at Joya de Ceren. *In* P.D. Sheets and S.E. Simmons, Eds., *Ceren Project 1993 Preliminary Report,* pp. 24–30. Boulder: Department of Anthropology, University of Colorado.
Olhoeft, G.R. (1981). Electrical Properties of Rocks. *In* W.R. Touloukian, W.R. Judd, and R.F. Roy, Eds., *Physical Properties of Rocks and Minerals,* pp. 257–330. New York: McGraw-Hill.
Olhoeft, G.R. (1984). Applications and Limitations of Ground-Penetrating Radar. *In Expanded Abstracts of the 54th Annual SEG International Meeting and Exposition,* pp. 147–148. December 2–6, Atlanta, Georgia.
Olhoeft, G.R. (1994). Modeling Out-of-plane Scattering Effects. *In Proceedings of the Fifty International Conference on Ground Penetrating Radar, June 12–16, Kitchener, Ontario, Canada,* pp. 133–144. Waterloo, Canada: Waterloo Centre for Groundwater Research.
Roosevelt, A.C. (1991). *Moundbuilders of the Amazon: Geophysical Archaeology on Marajo Island, Brazil.* New York: Academic Press.
Sellman, P.V., Arcone, S.A., and Delaney, A.J. (1983). Radar Profiling of Buried Reflectors and the Ground Water Table. *Cold Regions Research and Engineering Laboratory Report* **83–11,** 1–10.
Sheets, P.D. (1983). Introduction. *In* P.D. Sheets, Ed., *Archaeology and Volcanism in Central America,* pp. 1–13. Austin: University of Texas Press.
Sheets, P.D. (1992). *The Ceren Site: A Prehistoric Village Buried by Volcanic Ash in Central America.* Fort Worth: Harcourt Brace Jovanovich.
Sheets, P.D., Loker, W.M., Spetzler, H.A.W., and Ware, R.W. (1985). Geophysical Exploration

for Ancient Maya Housing at Ceren, El Salvador. *National Geographic Research Reports* **20,** 645–656.
Stove, G.C., and Addyman, P.V. (1989). Ground Probing Impulse Radar: An Experiment in Archaeological Remote Sensing at York. *Antiquity* **63,** 337–342.
Vaughan, C.J. (1986). Ground-penetrating Radar Surveys Used in Archaeological Investigations. *Geophysics* **51**(3), 595–604.
Vickers, R.S. and Dolphin, L.T. (1975). A Communication on an Archaeological Radar experiment at Chaco Canyon, New Mexico. *MASCA Newsletter* **11**(1).
Zier, C.J. (1983). The Ceren Site: A Classic Period Maya Residence and Agricultural Field in the Zapotitan Valley of El Salvador. *In* P.D. Sheets, Ed., *Archaeology and Volcanism in Central America,* pp. 119–143. Austin: University of Texas Press.

Received February 21, 1995
Accepted for publication March 6, 1995